LONGITUDINAL WAVE PROPAGATION IN A VISCOELASTIC SEMISPACE INCLUDING AN ABSORBING LAYER

K. S. Sultanov

UDC 622.026+650.834

In [1] Lyakhov proposed a model for rocks and soils which considers two limiting nonlinear compression diagrams; static (as $\dot{\varepsilon} \to 0$) and dynamic (as $\dot{\varepsilon} \to \infty$), as well as diagrams defining unloading of the medium. These diagrams refer to a single-axis deformed state, while deformation is regarded as having a volume nature.

In the case of longitudinal (weak) waves it can be proposed that residual deformations do not develop, and that static and dynamic compression diagrams are linear. With such assumptions the model of massive media with consideration of volume viscosity and plasticity [1] transforms to a model of a linear viscoelastic medium. The problems of shock wave interaction with viscous media with an undeformed boundary, movable or immobile, have been considered with this model previously [2, 3]. Questions of damping of seismic waves which develop in intense explosions and earthquakes lead to the problem of passage of longitudinal waves through an absorbing layer. Below we will present a solution to the problem of longitudinal wave propagation in a viscoelastic semispace containing an absorbing layer or obstacle. The solution is obtained by the characteristic method using a computer and the calculation technique presented in [1, 4].

The principles of longitudinal wave propagation in homogeneous viscoelastic media were considered in [5-7]. Wave problems for elastic layered media were considered in [8-11].

Problem Formulation and Method of Solution. The pattern for calculation in Lagrangian variables (h, mass; t, time) is presented in Fig. 1. We consider the semispace including the layer $h_1 - h_2$. The equations of state of the semispace and layer are considered linearly viscoelastic, but with differing physicomechanical characteristics. Below the subscripts i = 1, 2, 3 will refer to the medium ahead of the layer, the layer, and the medium beyond the layer.

The behavior of a linear viscoelastic medium (standard linear body) is defined by the equation

$$\dot{\varepsilon}_i + \mu_i \varepsilon_i = \dot{\sigma}_i / E_{Di} + \mu_i \sigma_i / E_{si}, \quad \mu_i = E_{Di} E_{si} / (E_{Di} - E_{si}) \eta_i, \tag{1}$$

where σ_i and ε_i are the longitudinal components of the stress and deformation tensors; E_{Di} is the dynamic compression modulus, and E_{si}, the static; η_i is the volume viscosity coefficient; μ_i, viscosity parameter; $\dot{\varepsilon}_i = d\varepsilon_i/dt$; $\dot{\sigma}_i = d\sigma_i/dt$.

A wave is created in the initial section h = 0 by a load varying by the law

$$\sigma_1 = \sigma_{max} \sin (\pi t/\theta) \quad \text{for } 0 \leqslant t \leqslant \infty, \tag{2}$$

where σ_{max} is the maximum value of the load; θ is the oscillation semiperiod. The oscillation frequency $f = 1/(2\theta)$ and $\omega = \pi/\theta$.

From the initial section an incident wave propagates, corresponding to the region 1 in the h, t plane (Fig. 1). The velocity of the incident wave front is c_{01}. After the incident wave reaches the layer at $h = h_1$ a reflected wave is formed (region 2), which in turn is reflected from the initial section h = 0, forming region 6, etc. The propagation velocity of all fronts ahead of the layer is equal to $c_{0.1}$. When the incident wave interacts with the layer there is formed in the latter a transmitted wave (region 3), with front velocity c_{02}. After the transmitted wave reaches the rear boundary of the layer h_2, a reflected wave is formed (region 4) together with a wave radiated into the medium behind the layer (region 5). The velocity of all fronts in the layer is equal to c_{02}. The velocity of the radiated wave front is c_{03}. After further multiple reflection and refraction regions 7-10, etc. are formed.

Tashkent. Translated from Zhurnal Prikladnoi Mekhaniki i Tekhnicheskoi Fiziki, No. 5, pp. 137-142, September-October, 1984. Original article submitted July 24, 1983.

 0021-8944/84/2505-0790$08.50

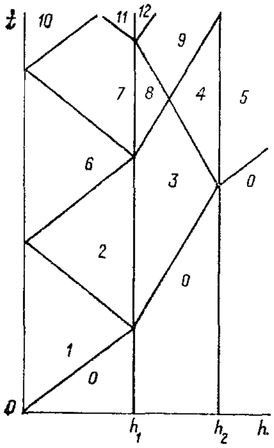

Fig. 1

The basic equations of medium motion in Lagrangian variables have the form

$$\partial u_i/\partial t - \partial\sigma_i/\partial h = 0,\quad \partial u_i/\partial h - \partial\varepsilon_i/\rho_0\partial t = 0, \tag{3}$$

where u_i is the particle velocity (mass velocity); ρ_{0i} are the initial densities of the media.

Solution of the problem reduces to integration of system (3) in each medium, complemented by Eq. (1) and boundary conditions; in the initial section Eq. (2) is satisfied, while on the incident and transmitted fronts where the viscous properties of the medium do not manifest themselves,

$$\sigma_i = -c_{0i}\rho_{0i}u_i = 0,\quad u_i = -c_{0i}\varepsilon_i = 0,\quad c_{0i} = \sqrt{E_{Di}/\rho_{0i}}, \tag{4}$$

where c_{0i} is the velocity of the beginning of the perturbation (front) defining the dynamic compression diagram. On the medium boundaries h_1 and h_2 the continuity condition

$$\sigma_1 = \sigma_2,\quad u_1 = u_2 \text{ and } \sigma_2 = \sigma_3,\quad u_2 = u_3 \tag{5}$$

is satisfied.

System (3), complemented by Eq. (1), is hyperbolic, with characteristic relationships in the form

$$d\sigma_i \mp c_{0i}\rho_{0i}du_i = -c_{0i}^2\rho_{0i}g(\sigma_i, \varepsilon_i)\,dt \quad \text{for} \quad \dot h = \pm c_{0i}\rho_{0i}, \tag{6}$$

$$d\sigma_i - c_{0i}^2 d\varepsilon_i = -c_{0i}^2\rho_{0i}g(\sigma_i, \varepsilon_i)\,dt \quad \text{for} \quad \dot h = 0,$$

$$g(\sigma_i, \varepsilon_i) = \sigma_i/\eta_i - E_{Di}E_{si}(\varepsilon_i - \sigma_i/E_{Di})/(E_{Di} - E_{si})\eta_i.$$

We will transform to dimensionless Lagrangian variables and dimensionless parameters

$$x = \mu_1 h/c_{01}\rho_{01},\quad \tau = \mu_1 t,\quad \sigma_i^0 = \sigma_i/\sigma_{\max},\quad \varepsilon_i^0 = \varepsilon_i/\varepsilon_{m1}, \tag{7}$$

$$u_i^0 = u_i/u_{m1},\quad \varepsilon_{m1} = \sigma_{\max}/E_{D1},\quad u_{m1} = -\sigma_{\max}/c_{01}\rho_{01}.$$

In these variables the initial equations take on the form

$$\frac{\partial u_i^0}{\partial\tau} + \frac{\partial\sigma_i^0}{\partial x} = 0,\quad \frac{\partial u_i^0}{\partial x} + p_i^2\frac{\partial\varepsilon_i^0}{\partial\tau} = 0,$$

$$\dot\varepsilon_i^0 + p_i\varepsilon_i^0 = \dot\sigma_i^0 + p_i\gamma_i\sigma_i^0;\quad p_i = \mu_i/\mu_1,\quad \gamma_i = E_{Di}/E_{si}.$$

As $\gamma_i \to 1$ the equation of state of the medium transforms to the equation of a Hook elastic medium.

The boundary conditions are as follows:

$$\sigma_1^0 = \sin \omega^0 \tau \quad \text{for} \quad x = 0 \ \text{and} \ 0 \leqslant \tau \leqslant \infty, \tag{8}$$
$$\sigma_i^0 = \varepsilon_i^0 = u_i^0 = 0 \quad \text{for} \quad x = k_i \tau,$$

where ω^0 is the dimensionless circular frequency, $\omega^0 = \pi/\mu_1\theta = \omega/\mu_1$; $k_i = c_{0i}\rho_{0i}/c_{01}\rho_{01}$. On the boundary between media $\sigma_1^0 = \sigma_2^0$ and $u_1^0 = u_2^0$; $\sigma_2^0 = \sigma_3^0$ and $u_2^0 = u_3^0$.

The characteristic relationships are:

$$d\sigma_i^0 \pm k_i du_i^0 = \left(\varepsilon_i^0 - \gamma_i \sigma_i^0\right) p_i d\tau \quad \text{along lines} \quad dx = \pm k_i d\tau,$$
$$d\sigma_i^0 - d\varepsilon_i^0 = \left(\varepsilon_i^0 - \gamma_i \sigma_i^0\right) p_i d\tau \quad \text{along lines} \quad dx = 0.$$

Upon transition from one medium to another the slope of the characteristics changes just like the wave front lines. For all media the time and spatial coordinate remain common in both dimensional and dimensionless variables. Dedimensionalizing Eqs. (1)-(6) with the aid of the dimensionless variables and quantities of Eq. (7) causes the dimensionless values σ_i^o and u_i^o for all media to be interchangeable, while ε_i^o are not interchangeable, since after dedimensionalization with the parameters of the first layer after simple transformations of Eq. (6) we obtain $\varepsilon_1^o = \varepsilon_1/\varepsilon_{m1}$, $\varepsilon_2^o = \varepsilon_2/\varepsilon_{m2}$, and $\varepsilon_3^o = \varepsilon_3/\varepsilon_{m3}$. The deformations obtained for the various layers are comparable only in dimensional values.

Wave parameters in the media depend on 19 dimensional constants E_{Di}, E_{Si}, η_i, ρ_{oi}, c_{oi}, σ_{max}, θ, h_1, h_2 ($i = 1, 2, 3$). Upon transition to dimensionless variables the problem contains 12 dimensionless parameters $\mu_1\theta$, γ_i, k_i, p_i, x_1, and x_2. This permits applying the results of one variant of computer calculation in dimensionless variables to a number of combinations of dimensional problem constants.

Calculation Results and Analysis. Calculations were performed on a BÉSM-6 computer for the variants presented in Table 1. The choice of variants was based on available experimental values of the dimensional constants. In soils γ varied from 1.5 to 5, and μ from 150 to 1500 sec^{-1} [1]. For rock γ lies in the interval from 1 to 3 and μ from 10^4 to 10^8 sec^{-1} [1, 12, 13]. If the value of μ_1 is taken equal to 10^3 sec^{-1}, then the table values correspond to a quite wide range of initial load frequencies, i.e., from 0.05 to 50 sec^{-1}, and for $\mu_1 = 10^4$ sec^{-1}, from 0.5 to 500 sec^{-1}.

We will consider the properties of the medium identical before and after the layer, so that $k_1 = k_3 = 1$ and $\gamma_1 = \gamma_3$. To reduce the number of variants we will take $p_i = k_i$. If $\gamma_2 > \gamma_1$, we obtain the problem of longitudinal wave propagation in a semispace containing an absorbing layer, since increase in γ corresponds to an increase in the difference between dynamic and static compression diagrams, i.e., to an increase in the medium's absorption coefficient and decrease in perturbation propagation velocity [7]. For the case $\gamma_1 = \gamma_2 = \gamma_3 = \gamma$ we obtain a homogeneous semispace. If $\gamma_2 < \gamma_1$, we have a semispace which contains a deformable obstacle.

The general principle of longitudinal wave propagation in media can be considered with the example of variant 3 (Fig. 2). Curves 0-7 represent dimensionless distances x, equal to 0, 3, 5, 7, 10, 18, 26, 34. The layer boundaries are located in the sections $x_1 = 5$ and $x_2 = 10$. The specified loading, creating a wave in the initial section, is steady state and according to Eq. (8) changes sinusoidally (curve 0). In the other sections, as is evident from Fig. 2, the variation of σ^0 with time is not steady state.

In all sections the maximum stress σ_m^o for the first passage of the wave is greater than on subsequent passages. The time required for the first passage σ_m^o increases with removal from the initial section, i.e., increases with x. When the wave passes through the layer the values of σ_m^o beyond the layer for the first passage and subsequent passages vary depending on the layer parameters. In all variants considered the functions $\sigma_m^o(x)$ were constructed from values of σ_m^o for the first arrival of the wave.

The effect of the ratio of the moduli of dynamic and static compression of the layer ($\gamma_2 = E_{D2}/E_{S2}$) on values of σ_m^o in media with $\mu_1\theta = 10$, $x_1 = 5$, and $x_2 = 10$ are presented in Fig. 3. Here and in subsequent figures the curves are numbered in correspondence with the enumeration of Table 1. The γ_2 values chosen for variants 1-4 correspond to media which

TABLE 1

Variant No.	$\mu_1 0$	γ_1, γ_3	γ_2	k_2	x_1	x_2	Variant No.	$\mu_1 0$	γ_1, γ_3	γ_2	k_2	x_1	x_2
1	10	1,1	2	0,8	5	10	14	10^2	1,1	4	0,5	100	200
2	10	1,1	4	0,6	5	10	15	10	2	4	0,8	5	10
3	10	1,1	4	0,5	5	10	16	10	2	4	0,6	5	10
4	10	1,1	4	0,2	5	10	17	10	1,02	4	0,6	5	10
5	10	1,1	4	0,5	50	70	18	10	1,02	2	0,6	5	10
6	10^2	1,1	4	0,5	50	70	19	10^2	1,02	4	0,6	5	10
7	$3 \cdot 10^2$	1,1	4	0,5	50	70	20	10^2	2	1,02	2,0	5	10
8	$5 \cdot 10^2$	1,1	4	0,5	50	70	21	10^3	2	1,02	2,0	5	10
9	10^3	1,1	4	0,5	50	70	22	10	2	1,02	2,0	5	7
10	10^4	1,1	4	0,5	50	70	23	10	2	1,02	2,0	5	10
11	10^2	1,1	4	0,5	100	120	24	10	2	1,02	2,0	5	15
12	10^2	1,1	4	0,5	150	170	25	10	2	1,02	2,0	5	25
13	10^2	1,1	4	0,5	200	220							

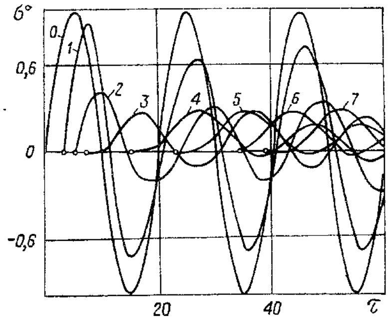

Fig. 2

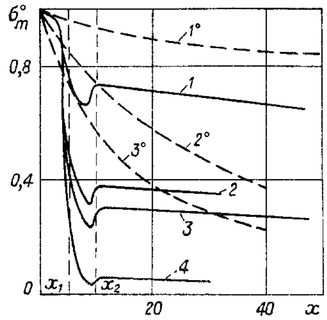

Fig. 3

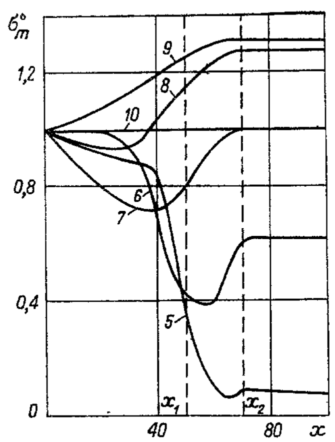

Fig. 4

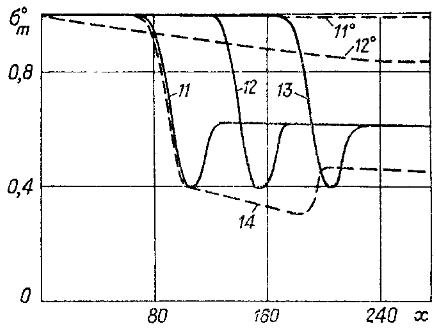

Fig. 5

absorb as compared to the media ahead of and behind the layer. Moreover, one and the same γ_2 may correspond to different k_2, since γ_2 is the ratio of E_{D2} to E_{S2}. Decrease in k_2 at constant γ_2 corresponds to a decrease in wave impedance of the layer or decrease in wave propagation velocity within the layer.

Curves 1°-3° in Fig. 3 show the functions $\sigma_m^o(x)$ at γ = 1.1; 2; 4 respectively ($\gamma_1 = \gamma_2 = \gamma_3 = \gamma$). In these cases the maximum dimensionless value of σ_m^o decreases monotonically with distance, and the greater the value of γ, the more intense the damping. Change in γ_2 at constant $\gamma_1 = \gamma_3$ changes the behavior of curves 1°-3°. With increase in γ_2 the value of σ_m^o begins to drop sharply in sections of the medium ahead of the layer and continues to fall in the initial sections of the layer itself (curves 1-4), since upon interaction with the absorbing layer the wave reflected from the layer is a rarefaction wave. When the incident wave front reaches the

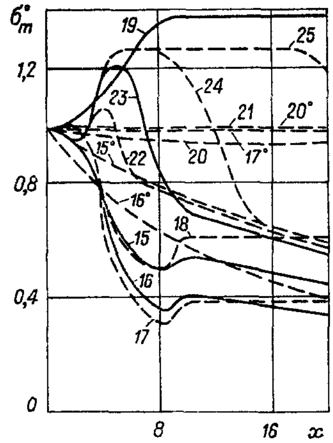

Fig. 6

back boundary of the layer a reflected compression wave appears. Superposition of the incident and reflected waves produces a rise in σ_m^o in the back sections of the layer. Further, at medium depths within the layer the changes in $\sigma_m^o(x)$ are analogous to curve 1°, but with a differing level of σ_m^o. By increasing the value of γ_2, i.e., choosing materials having different viscous properties, a greater reduction in stress beyond the layer can be achieved (curves 1, 2). Upon decrease in the propagation velocity of longitudinal waves within the layer, which corresponds to increase in porosity of the layer material, the value of σ_m^o beyond the layer increases even more (curves 3, 4). When the propagation velocity of the wave within the layer is equal to one-fifth of the velocity ahead of and beyond the medium ($k_2 = 0.2$), the value of σ_m^o beyond the layer is decreased by almost 95% (curve 4). It is evident from this that at some values of γ_2 and k_2 complete extinction of the wave passing through the layer can be achieved. However this depends on the frequency of the wave.

The effect on σ_m^o of the load oscillation frequency $f = 1/(2\theta)$ was considered with the calculations of variants 5-10 (Fig. 4). For constant $\mu_1 = 10^3$ sec^{-1} variants 5-10 (Fig. 4) describe waves with frequencies of 50, 5, 1.67, 1, 0.5, and 0.05 sec^{-1} respectively, while for $\mu_1 = 10^4$ sec^{-1} they refer to frequencies of 500, 50, 16.7, 10, 5, and 0.5 sec^{-1}. For these variants the layer boundaries are located in the sections $x_1 = 50$ and $x_2 = 70$ (dashed region in Fig. 4). For this case $\gamma_1 = \gamma_3 = 1.1$, $\gamma_2 = 4$, and $k_2 = 0.5$.

Upon passage of high-frequency waves through an absorbing layer the value of σ_m^o beyond the layer decreases significantly (curve 5). Decrease in wave frequency by a factor of 10 produces an increase in σ_m^o beyond the layer by a factor of approximately 6 times (curves 5 and 6). Further decrease in frequency changes the behavior of the $\sigma_m^o(x)$ curves intensely. Upon passage of low-frequency waves through an absorbing layer the wave process develops slowly and is quasistatic. In these cases during the time required for passage of the wave the absorbing layer deforms significantly, as a result of which the value of σ_m^o in the layer increases (curves 8, 9). For very-low-frequency waves the layer has no effect on wave parameters (curve 10).

The ratio of wavelength λ to layer thickness r is defined in terms of the dimensionless parameters as $\lambda/r = 2\mu_1\theta/(x_2 - x_1)$.

In variants 5-10 considered in Fig. 4 the ratio λ/r is equal to 1, 10, 30, 50, 100, and 1000. It is evident from Fig. 4 that at a value of $\lambda/r < 30$ the wave parameters beyond the layer attenuate, while for $\lambda/r \geqslant 30$ they either increase or remain unchanged. Other conditions being equal, to achieve more effective wave damping beyond the layer it is necessary to determine the layer thickness from the condition $r = 0.1\lambda$, m.

Removal of the layer from the initial section causes a reduction in the value of σ_m^o beyond the layer (curve 3 of Fig. 3 and curve 5, Fig. 4). However this phenomenon is observed only for high frequency waves at $\lambda/r < 10$.

The effect of dimensionless distance x_1 on the value of σ_m^o beyond the layer at constant layer thickness for $\lambda/r = 10$ is shown in Fig. 5. Here $\mu_1\theta = 100$, $\gamma_1 = \gamma_2 = 1.1$, $\gamma_2 = 4$, $k_2 = 0.5$. Curves 11° and 12° show $\sigma_m^o(x)$ in a homogeneous medium at $\gamma = 1.1$ and 4, with $\mu_1\theta = 100$.

In these cases the distance from the original section to the leading edge of the layer x_1 or location of the absorbing layer does not affect the value of σ_m^o beyond the layer (curves

11-13). The behavior of the curves $\sigma_m^o(x)$ for variants 11-13 is similar to the $\sigma_m^o(x)$ curves considered in Fig. 3.

With increase in layer thickness, which also corresponds to reduction in the ratio λ/r, the value σ_m^o decreases during wave propagation in the absorbing layer itself, which leads to a higher value of σ_m^o beyond the layer (curve 14).

The effect of change in γ_1 and γ_3 as well as γ_2 on the function $\sigma_m^o(x)$ is shown in Fig. 6. Curves 15°-17° and 20° describe damping of the maximum stress at fixed locations in a homogeneous medium ($\gamma_1 = \gamma_2 = \gamma_3 = \gamma$) at $\mu_1\theta = 10$ and $\gamma = 2, 4, 1.02$ (curves 15°-17°, respectively). Curve 20° is for $\gamma = 1.02$ and $\mu_1\theta = 100$.

For $\lambda/r < 10$ changes in γ_1 and γ_3 have an insignificant effect on σ_m^o beyond the layer (curve 2, Fig. 3 and curves 16, 17, Fig. 6). The quantities γ_2 and k_2 begin to affect stress damping beyond the layer here (curves 15, 17, 18). Increase in wave frequency also changes the behavior of $\sigma_m^o(x)$ (curves 17 and 19).

For the case $\gamma_2 > \gamma_1 = \gamma_3$ the layer becomes a deformable obstacle. If we take $\gamma_2 = 1.02$, then we have an elastic obstacle located in a viscoelastic semispace. Screening of longitudinal waves by an elastic obstacle was studied with variants 20-25. As is evident from the calculation results, after passage through an elastic obstacle longitudinal waves maintain practically the same σ_m^o value beyond the obstacle as in the absence of the obstacle (curves 20° and 20, 21). At very low frequencies the longitudinal waves scarcely "notice" the elastic obstacle (curves 20° and 21).

The principles of change of the parameters u_m^o and ε_m^o upon passage of longitudinal waves through an absorbing layer or elastic obstacle in a semispace are analogous to the changes in σ_m^o presented in Figs. 2-6.

Thus, the parameters of longitudinal waves in a semispace vary in the presence of an absorbing layer as functions of the physicomechanical properties and thickness of the layer, as well as incident wave frequency. In propagation of longitudinal waves in linear layered inhomogeneous viscoelastic media at certain ratios of wavelength to layer thickness the absorbing medium plays the role of a frequency filter. Longitudinal waves are attenuated insignificantly on passage through elastic obstacles.

LITERATURE CITED

1. G. M. Lyakhov, Fundamentals of Explosive Waves in Soils and Rocks [in Russian], Nedra, Moscow (1974).
2. G. M. Lyakhov and K. S. Sultanov, "Wave interaction with an obstacle with consideration of volume viscosity of the soil," Fiz. Goreniya Vzryva, No. 4 (1977).
3. G. M. Lyakhov and K. S. Sultanov, "Wave interaction in a viscoplastic medium with an obstacle," Zh. Prikl. Mekh. Tekh. Fiz., No. 4 (1978).
4. N. E. Hoskin, "The characteristic method for solution of one-dimensional nonsteady state flow equations," in: Computation Methods in Hydrodynamics [Russian translation], Mir, Moscow (1974).
5. S. Ya. Kogan, "Brief review of seismic wave absorption theories," Izv. Akad. Nauk SSSR, Fiz. Zeml., No. 11 (1966).
6. G. Rodin, Seismology of Nuclear Explosions [Russian translation], Mir, Moscow (1964).
7. G. M. Lyakhov and K. S. Sultanov, "Longitudinal waves in linear viscoelastic media", Izv. Akad. Nauk SSSR, Fiz. Zeml., No. 8 (1978).
8. L. M. Brekhovskikh, Waves in Layered Media [Russian translation], Mir, Moscow (1973).
9. N. A. Shul'ga, "Elastic wave reflection from an orthotropic regularly layered semispace," Prikl. Mekh. 15, No. 5, (1979).
10. N. A. Shul'ga and V. M. Antonenko, "Wave propagation across a multicomponent layered composite structure", direction," Prikl. Mekh. 18, No. 2 (1982).
11. S. T. San, J. Achenbach, and G. Gerrman, "Harmonic waves in a layered medium propagating in the layered direction," Trans., AIME, No. 2 (1969).
12. B. P. Belikov, K. S. Aleksandrov, and T. V. Ryzhova, "Elastic Properties of Powder-forming Minerals in Rocks [in Russian], Nauka, Moscow (1970).
13. G. Duvall, "Propagation of plane shock waves in a stress-relaxing medium," in: Stress Waves in Anelastic Solids, Berlin (1964).